Shining light on sky cover during a total solar eclipse

Jordan J. Gerth

Shining light on sky cover during a total solar eclipse

Jordan J. Gerth*

University of Wisconsin–Madison, Cooperative Institute for Meteorological Satellite Studies, Space Science and Engineering Center, Madison, Wisconsin, United States

Abstract. Sky cover is a unique parameter because its quantification is subject to the perspective of the observer or characteristics of the observing instrumentation. Forecasting sky cover provided a professional challenge to operational meteorologists seeking to offer a refined forecast beyond numerical weather prediction guidance along the path of totality resulting from a solar eclipse traversing North America on August 21, 2017. A routine analysis with which to monitor subtle trends in sky cover and compare sky cover forecasts is also not widely available. This contribution reviews 1-h gridded forecasts of sky cover from the United States National Weather Service (NWS) on the eclipse day and compares them with hourly satellite and surface sky observations for an area of interest over the southeastern United States. An inconsistency between the real-time mesoscale analysis (RTMA) and the NWS National Digital Forecast Database is revealed during the eclipse totality. A satellite-to-satellite comparison of the adjusted average cloud top emissivity over this same area reveals how resolution and algorithm improvements to next-generation satellite imagers may alter the RTMA of total cloud cover in the latest era of Geostationary Operational Environmental Satellites (GOES), starting with the GOES-16 Advanced Baseline Imager. © *The Authors. Published by SPIE under a Creative Commons Attribution 3.0 Unported License. Distribution or reproduction of this work in whole or in part requires full attribution of the original publication, including its DOI.* [DOI: 10.1117/1.JRS.12.020501]

1 Introduction

Ahead of the solar eclipse of August 21, 2017, with a path of totality that crossed the United States from Oregon to South Carolina, interested Americans and international tourists seeking to observe the eclipse needed to find a cloud-free viewing location. This increased public interest for sky cover climatologies and forecasts, which typically have more specialized applications. In the Federal Meteorological Handbook No. 1, sky cover is defined as "the amount of the celestial dome hidden by clouds and/or obscurations."[1] The difference between sky cover and cloud fraction is the frame of reference. Sky cover can be thought of as cloud fraction over the entire celestial dome, from the perspective of a point observer. Similar clouds obscure the celestial dome differently depending on their extent and position relative to the observer. In contrast, numerical weather prediction (NWP) models provide total and layer cloud cover fields, which are calculated based on the fractional cloud coverage of a grid cell, and, for some NWP models, are smoothed horizontally to better approximate a celestial dome. As discussed further in Appendix A.1, there are several diagnostic approaches to calculating cloud fraction fields from prognostic variables in NWP models.

In providing sky cover forecasts to the public, United States National Weather Service (NWS) meteorologists introduce NWP cloud fraction fields into the sky cover grid of the National Digital Forecast Database (NDFD).[2] Each NWS forecast office contributes a geographic section known as the forecast area of responsibility to the NDFD grid as part of routine

---

*Address all correspondence to: Jordan J. Gerth, E-mail: jordan.gerth@ssec.wisc.edu

shift duties. NDFD grids are inherited from previous shifts and can be updated many times throughout a shift. Though NWS meteorologists can use guidance fields directly from a single NWP model, they routinely blend guidance from multiple models, use precalculated statistical blends,[3] or make adjustments based on observations, independent of frequent analyses or short-term forecasts from NWP models, in the interest of collaboration and producing a consistent forecast. The NDFD provides the best human assessment and representation of meteorological parameters and their forecasted state.

Meteorologists can monitor the hourly real-time mesoscale analysis (RTMA),[4] which ingests satellite and *in-situ* surface sky observations, for current conditions to maintain a representative short-term forecast. Although both satellite and surface observations are integral to the development of the RTMA total cloud cover analysis, combining these different types of observations is complicated due to different viewing geometries, complex spatial scales, and varying relative frequencies. More detail about the creation of the RTMA total cloud cover analysis, which uses an operational NWP model forecast as a background, can be found in Appendix A.2. Operational NWP models have climatological and diurnal adjustments to the solar radiative forcing, but they do not account for decreases in shortwave radiation as the result of an eclipse, though an experimental version of the High-Resolution Rapid Refresh (HRRR) did.[5]

The additional, albeit predictable, variability of incoming solar radiation resulting from an eclipse can increase the challenge of quantifying and forecasting sky cover, as this article will discuss. The evolution and extent of the cloud field, in terms of sky cover and cloud fraction, over a portion of the southeastern United States on the day of the eclipse, August 21, 2017, is studied here. As part of the study, this article compares the visible satellite imagery and surface sky observations with the RTMA total cloud cover analysis, relying on geostationary satellite imager input and NDFD 1-h forecast of sky cover for the area of interest between 1700 and 2100 UTC, which is around and shortly after solar noon.

The purpose of the study is to review the short-term NDFD forecasts for the episode and highlight ongoing uncertainty about quantifying sky cover as a meteorological parameter. In doing so, the change in sky cover over time during the passage of the solar eclipse is examined for the surface observations, RTMA fields, and NDFD 1-h forecasts. To limit the contributions of scale-dependent forcing mechanisms for clouds (e.g., synoptic scale weather systems resulting in broader, deeper ascent) beyond the background thermodynamics, the area of interest was selected based on the predominant presence of diurnal cumulus clouds, but no deep convective cloud, on the day of the eclipse.

The passage of totality, resulting in the most significant decrease in incoming solar radiation, also intersected the area of interest. There were eclipse effects on clouds outside this area, though the extent of those effects depended on the antecedent meteorological conditions and the time of day of the eclipse passing. Similar effects on the cumulus cloud field as presented in this article were evident from portions of southern Ontario in Canada to southern Texas in the United States. Where a cumulus cloud field was not established prior to the beginning of the eclipse, such as in the northwestern contiguous United States, or where deep convective cloud had developed, such as over the Northern Plains of the United States, the eclipse effects on cloudiness were uncertain.

2 Discussion

This study introduces a methodology for gridding sky observations such that a comparison with meteorological satellite imagery and derived sky products is possible. The gridded sky observations are then used for comparison with other analyses and forecasts for the area of interest. In particular, the RTMA is used to demonstrate the added value of satellite observations in quantifying sky cover.

2.1 *Surface Sky Observations*

Distilling surface sky cover observations into a percentage based on coded Meteorological Terminal Aviation Routine Weather Reports (METARs) cannot be done in a precise manner for multiple reasons. First, while surface weather stations have ceilometers to help with the

estimation of cloud base height, human observers may opt to augment these reports at some stations, but there is no report indicator or practical method to assess whether this is done regularly or if the skill of different human observers at augmenting the instrumentation is good. Though darkness can increase challenges for observers estimating cloudiness overnight compared with during the day, an observer's skill during a partial eclipse would likely compare with other daytime observations. Given that totality lasted under 3 min, the careful observer could easily assess cloudiness before and after the total eclipse if the unique illumination of the horizon made it challenging to ascertain clouds. Second, automated ceilometer reports use a time average from a point, which is typically preferential to low clouds, or clouds directly over the ceilometer, instead of capturing the entire celestial dome. A stationary cloud over a surface station ceilometer may lead to an overrepresentation of sky cover in the respective observation. Third, while cloud cover is observed in oktas, or one-eighth increments of fractional coverage, coded METARs constrain the observation to one of the five groups, CLR (clear), FEW (few), SCT (scattered), BKN (broken), and OVC/VV (overcast, or vertical visibility obscured).[1]

For this study, the routine and special METARs were decoded and binned to a 10-km Lambert Conformal grid and, by bin, averaged over a 1-h window bounded by the top of the hours adjacent, with sky conditions assigned 0%, 25%, 40%, 75%, and 100% for the five progressively greater METAR cloud coverage groups, following an approach from the General Meteorological PAcKage, or GEMPAK software.[6] The binning occurred in both time and space; however, the selection of the 10-km grid generally precluded the inclusion of more than one observation site in a grid cell, with very limited exception. Both automated and manual reports were binned, but routine observations for this study do not include those at a frequency of 1 or 5 min. These binned observations were then compared with visible satellite
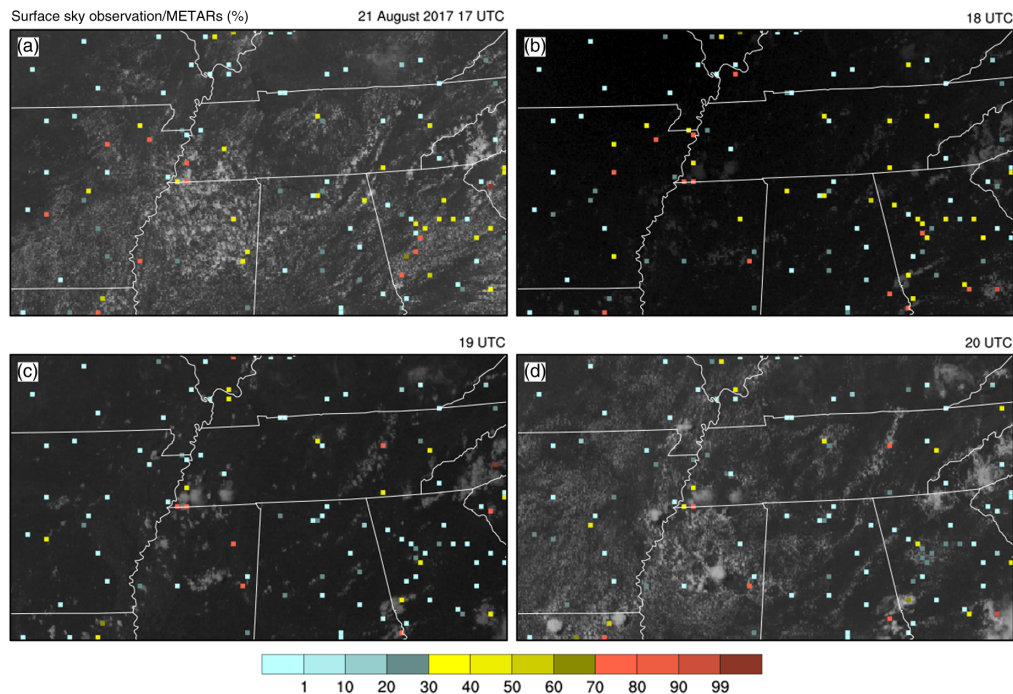
Fig. 1 Surface sky observations. This four-panel plot shows decoded, binned, and averaged surface sky observations, in units of percent (%) coverage, on a 10-km Lambert Conformal grid over a portion of the southeastern United States for the 1-h period following (a) 1700 UTC, (b) 1800 UTC, (c) 1900 UTC, and (d) 2000 UTC on August 21, 2017, in the respective panels. Similarly, the underlying visible satellite images from a Geostationary Operational Environmental Satellite, GOES-13, are valid at (a) 1700 UTC, (b) 1815 UTC, (c) 1900 UTC, and (d) 2000 UTC on August 21, 2017. The satellite images are darker in the top-right and bottom-left due to the proximity in time to totality from the solar eclipse, which decreased incoming solar radiation, though less cloudiness was also evident.

imagery from the eastern United States Geostationary Operational Environmental Satellite (GOES-13), valid at or shortly after the top of the hour, when most of the observations were made, as shown in Fig. 1.

Visible images from the GOES-16 Advanced Baseline Imager (ABI), which was not yet operational at the time of the eclipse but has two visible wavelength bands for monitoring clouds during the day, are similar. The lunar umbra and penumbra from the eclipse were also clearly evident in the ABI near-infrared bands, particularly the 0.86-μm vegetation band,[7] though the relatively high reflectance of land surfaces at that wavelength makes cloud detection more challenging. The presence of cloud on satellite imagery adequately corresponds to the gridded surface sky observations, though the coverage accuracy is difficult to assess other than subjectively.

2.2 Comparisons and Trends

An hourly comparison of the mean of the stations shown in Fig. 1 is shown in Table 1 for each 1-h window between 1700 and 2100 UTC, along with the satellite-surface RTMA mean and human NDFD 1-h forecast grid mean for the corresponding four times. Between 1700 and 1800 UTC, the mean sky cover reported in surface observations was consistent with the mean value from the NDFD 1-h forecast grid, though that correspondence diverged for the remainder of the period of interest. The time of totality in the vicinity of Nashville, Tennessee, was around 1830 UTC. There was a minimum in mean total cloud cover from the RTMA at 18 and 19 UTC that was not reflected in the NDFD 1-h forecast grid mean and that preceded the minimum in the surface sky observations mean. The latter is likely due to the collection of many observations from surface stations solely at the top of the hour.

A value-binned comparison of the surface sky observations and RTMA total cloud cover analysis mean with the NDFD 1-h sky cover forecast grid is shown in Figs. 2 and 3, respectively, for the 19 UTC time window, following the departure of the total eclipse for this area of interest. For this case, a high fraction of nonzero NDFD forecast sky cover values correspond to observed clear skies (i.e., a cloud cover of <5%), though this is particularly evident with the comparison with the RTMA. Almost all of the NDFD forecast values in the area of interest are greater than the corresponding RTMA cloud cover values at this time period.

This mean decrease in the RTMA is likely a result of the dense satellite observations, particularly because the RTMA mean was less than the surface sky observations mean. The location-specific 1-h differences between time-adjacent RTMA total cloud cover analyses are shown in Fig. 4. There was a decrease in cloud cover over northern Mississippi per the RTMA total cloud cover analysis from 17 to 18 UTC, as indicated in blue colors in Fig. 4(a), as the eclipse approached, and an increase in cloud cover from 19 to 20 UTC, as indicated in red colors in Fig. 4(c), when the eclipse effects waned. Cloudiness decreased substantially, in excess of 45%, over portions of northern Mississippi during the passage of the eclipse, and then rebounded later in the afternoon. The trend over time contrasts with the NDFD 1-h forecast grid adjacent hour differences, shown in Fig. 5. There are slight differences between NWS forecast areas of responsibilities but no evidence of occurring or anticipated eclipse effects in the NDFD forecast grid for the area of interest. This suggests that the NWS meteorologists monitoring the NDFD on the

Table 1 For 1-h increments between 1700 and 2100 UTC on August 21, 2017, this table summarizes the computed mean, in percent (%) coverage, for surface sky observations, the RTMA total cloud cover analysis, and the NDFD 1-h sky cover forecast grid. The geographic area of interest from which the mean was computed is shown in Fig. 1. The valid time range for each column is 1 h following the header time. Each NDFD forecast was issued 1 h prior to the header time; the mean was computed for the valid time.

August 21, 2017, sky cover	17 UTC (%)	18 UTC (%)	19 UTC (%)	20 UTC (%)
Surface sky observations mean	24	26	16	16
RTMA total cloud cover analysis mean	16	7	6	12
NDFD 1-h sky cover forecast grid mean	27	31	33	36

**Sky cover comparison
21 August 2017 19 UTC**
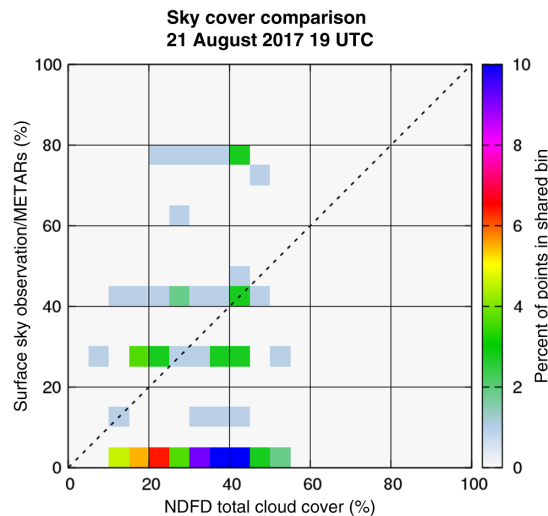
Fig. 2 Comparison of surface sky observations to the NDFD 1-h sky cover forecast. There were 110 comparisons of gridded automated and manual surface sky observations with the NDFD 1-h sky cover forecast in the domain of interest (as shown in Fig. 1) for the 1 h following 1900 UTC on August 21, 2017. Comparisons are plotted in bins of 5% that represent the percent of grid points in the corresponding range; each cell on the plot has edge dimensions of 5%. Cells to the left of the dashed line indicate where surface sky observation values are greater than NDFD sky cover forecast values; cells to the right of the dashed line are lesser than NDFD sky cover forecast values.

**Sky cover comparison
21 August 2017 19 UTC**
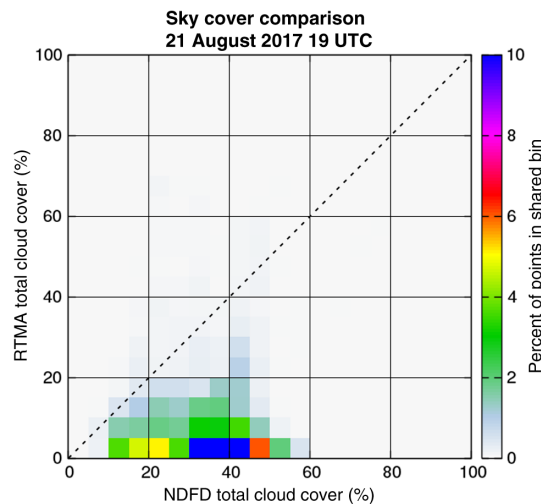
Fig. 3 Comparison of the RTMA cloud cover to the NDFD 1-h sky cover forecast. There were 6696 grid cell comparisons of RTMA total cloud cover field with the NDFD 1-h sky cover forecast in the domain of interest (as shown in Fig. 1) for the 1 h following 1900 UTC on August 21, 2017. Comparisons are plotted in bins of 5% that represent the percent of grid points in the corresponding range; each cell on the plot has edge dimensions of 5%. Cells to the right of the dashed line indicate those sky coverage categories where the NDFD sky cover forecast exhibits a high bias compared with the RTMA.

eclipse day either relied strongly on the operational NWP guidance that did not account for decreased incoming solar radiation during the eclipse, or they were uncertain about the magnitude and timing of the decrease in sky cover that the eclipse would produce, even as it was imminent and observable in visible satellite images (Fig. 1). The NWS does not provide information about the composition of specific NDFD grids and meteorologist modifications; those likely vary from office to office.
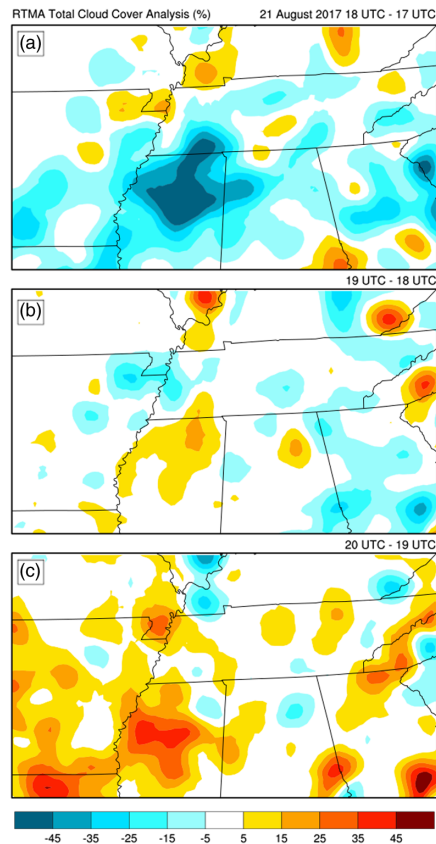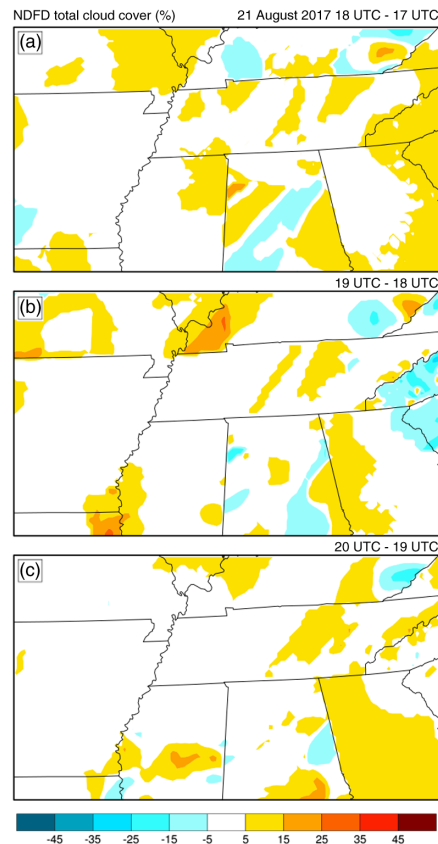
Fig. 4 RTMA total cloud cover analysis temporal differences. This three-panel plot shows the RTMA total cloud cover analysis temporal differences, in units of percent (%) coverage, on a 10-km Lambert Conformal grid between (a) 17 and 18 UTC, (b) 18 and 19 UTC, and (c) 19 and 20 UTC on August 21, 2017, in the respective panels. In each of the three panels, the earlier analysis valid time is subtracted from the later analysis valid time. Yellow areas show slight increases to the cloudiness during the respective time windows, whereas blue areas show decreases. The collection of analyses depicts decreasing cloudiness ahead of totality and increasing cloudiness following totality.

2.3 *Future of Satellite Sky Cover*

NWS meteorologists have access to weather satellite imagery and satellite-derived products. An infrared window band provides an alternative to a visible band for monitoring a solar eclipse, despite the nominal 2-km spatial resolution, because the radiating temperature of land surfaces decreases without incoming solar radiation and clouds are still evident regardless of the amount of solar illumination. The additional infrared window spectral bands and finer spatial resolution of the ABI on GOES-16 will improve the detection and characterization of clouds from the geostationary orbit.[8] To examine the quantitative value of increased-resolution infrared window radiances, the adjusted average cloud top emissivity (AACTE) fields from GOES-13, computed with data from the legacy imager, and GOES-16, with data from the ABI,[9] are compared, as shown in Fig. 6.

Infrared window radiances are used to calculate cloud top emissivity. Cloud top emissivity is also referred to as effective cloud amount because a cloud top emissivity of less than unity indicates that a cloud occupies a fraction of the pixel, the cloud is semiopaque, or a semiopaque cloud occupies a fraction of the pixel. The AACTE quantifies an otherwise subjective assessment of sky cover with a single time spatial average containing corrections in cases of multilayered cloud decks and some near-overcast homogeneous cloud decks.[10] The spatial average contains all pixels within a 25-km radius around a point. Near the satellite subpoint, there are more adjacent pixels incorporated into the AACTE for a given point than at latitudes and longitudes further

Fig. 5 NDFD sky cover forecast temporal differences. This three-panel plot shows the NDFD 1-h sky cover forecast grid temporal differences, in units of percent (%) coverage, on a 10-km Lambert Conformal grid between (a) 17 and 18 UTC, (b) 18 and 19 UTC, and (c) 19 and 20 UTC on August 21, 2017, in the respective panels. In each of the three panels, the earlier forecast valid time is subtracted from the later forecast valid time. Yellow areas show slight increases to the sky cover forecast during the respective time windows, whereas blue areas show decreases. A trend pattern between panels is not apparent. Each NDFD forecast was issued 1 h prior to the valid time. Differences aligned to political boundaries likely reveal different forecasts along adjacent office areas of responsibility.

from the subpoint. Because the cloud top emissivity is itself a spatial average, though becoming less so for higher resolution imagers such as the ABI, the additional smoothing effect of the AACTE does not lead to significantly degraded calculations at large viewing angles where pixels cover a broader spatial area than at the satellite subpoint. Although it is not possible to run the RTMA for this day with GOES-16 input, the AACTE would have been the principal input to the RTMA total cloud cover analysis had it not been preoperational.

The grid mean AACTE values over the interest area for 2000 UTC on the eclipse day, ~90 min after totality, are similar; the GOES-13 imager grid mean AACTE value is 16%, 3% greater than the mean from the GOES-16 ABI. Local differences are evident, most commonly and likely resulting from the nominal 2-km spatial resolution of the ABI infrared bands.[6] For mostly cloudy scenes, subpixel cloud breaks are less evident with the lower, 4-km resolution of the legacy imager. Conversely, the ABI can capture small clouds in otherwise mostly clear scenes. The result of this, as evident in Fig. 6(d), is that the mostly clear areas are cloudier in terms of AACTE when viewed with the ABI, such as over southwestern Kentucky, and partly/mostly cloudy areas are clearer, such as over northern Mississippi. There are also differences where semiopaque cirrus clouds are present, such as over southeastern Kentucky, based on improved cloud top height assignments with the additional ABI infrared window spectral bands.[9]
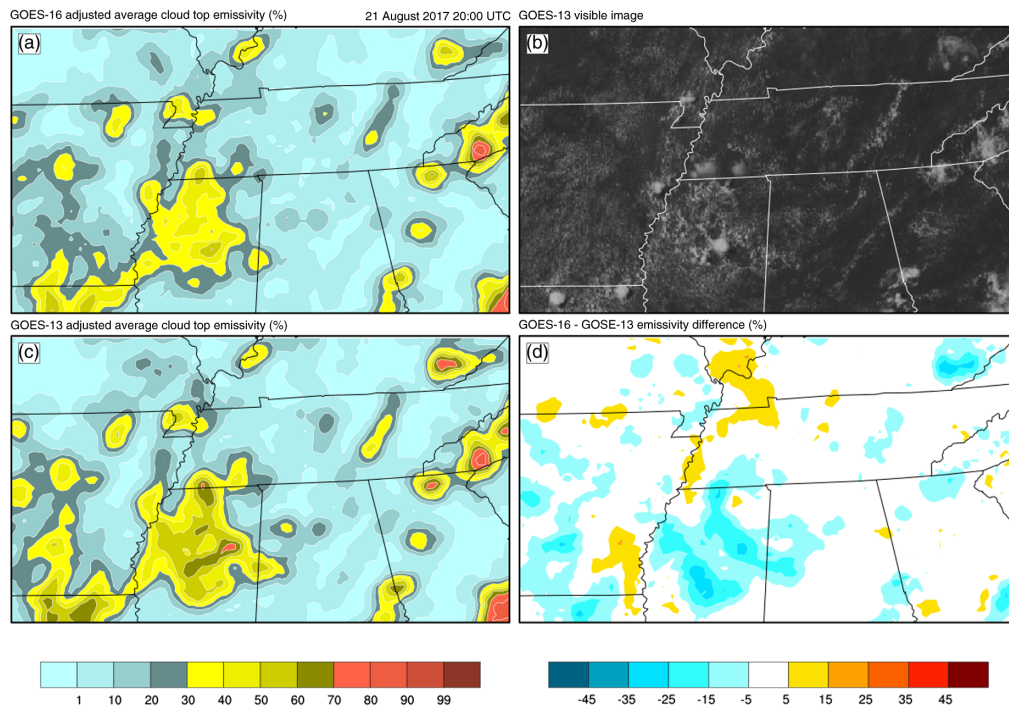
Fig. 6 Adjusted average cloud top emissivity. This four-panel plot provides a comparison between the adjusted average cloud top emissivity (AACTE), in units of percent (%), from two Geostationary Operational Environmental Satellites, (a) GOES-16 and (c) GOES-13, at 2000 UTC on August 21, 2017. A (b) visible image from GOES-13 at the same time assists in characterizing the scene, and the (d) AACTE difference of GOES-13 from GOES-16 reveals local contrasts between (a) GOES-16 and (c) GOES-13. Yellow (positive) areas generally show mostly clear areas where GOES-16 imagery input increased the areal emissivity calculation, whereas blue (negative) areas show cloudier areas where GOES-16 imagery input decreased the areal emissivity calculation. Some semiopaque cirrus clouds also have a greater AACTE with GOES-13 than GOES-16.

3 Conclusion

The presented analyses and forecasts of cloud and sky cover over the southeastern United States on August 21, 2017, highlight the challenges in forecasting sky cover during this unique event and finding a suitable representation of observed sky conditions. In particular:

- There are a limited number of point-based surface sky observations. They vary in precision, quality, and frequency and may not represent conditions for adjacent areas. This increases the value of satellite observations for the subjective monitoring of sky cover and development of derived products.
- The RTMA total cloud cover analysis captured, and quantified, the decrease in clouds observable with satellite imagery during the eclipse. Due to satellite observations, the mean RTMA cloud cover was considerably less than the mean from the NDFD 1-h sky cover forecasts for the area of interest, despite also incorporating surface sky observations.
- Despite public and international attention as a result of the eclipse, the NDFD 1-h sky cover forecasts did not capture the decrease in sky cover coincident with the minimum in incoming solar radiation as a result of the eclipse for this area of interest.
- Compared with GOES-13, the improved spatial and spectral resolution of the ABI will affect AACTE calculations for some cloudy scenes and therefore the RTMA total cloud cover analysis when GOES-16 is operational.

This is a single case, and comparisons between surface sky observations, RTMA total cloud cover analyses, and NDFD 1-h sky cover forecasts will likely vary daily, geographically, and

seasonally. Formalizing a common measure of sky cover based on more frequent surface sky observations, GOES-16 satellite imagery, and better satellite-cloud assimilation in high-resolution NWP models is a pragmatic first step ahead of the next total solar eclipse in North America that will occur on April 8, 2024.

Appendix A: RTMA Total Cloud Cover Analysis

A.1 Approaches to Quantifying Sky Cover

There are both prognostic and diagnostic approaches to cloud fraction.[11] Diagnostic equations are prevalent in real-time NWP guidance available operationally though, relying on relative humidity,[12] vertical velocity,[13] environmental stability,[14] and mean liquid water content[15] or a combination thereof. These approaches to cloud fraction are applied today because the scale of individual cloud processes is generally less than the grid spacing that operational models afford, though NWP models of increasingly high spatial resolution that explicitly allow convection are increasing in routine availability. The Weather Research and Forecast model still relies on the Xu and Randall scheme[15] as the default, with the Sundqvist et al. scheme[16] as an option. Furthermore, the parameters reflected in the diagnostic approaches are not immediately consequent to incoming solar radiation.

A.2 Construction of Sky Cover Field

The background sky cover field from the RTMA comes from the 1-h forecast of the HRRR[17] and, when unavailable, the Rapid Refresh (RAP).[17] Furthermore, in producing the total cloud cover field, the weight of the background HRRR/RAP field is minimal due to the density and weight of sky cover observations from the two Geostationary Operational Environmental Satellites (GOES),[18] in this case GOES-15/west and GOES-13/east. The RTMA ingests satellite-cloud amount information in the form of a sky cover product[8] as "data of opportunity," in addition to surface sky observations.[18] "Data of opportunity" is produced at a research center, where it may not be routinely monitored. In this case, the Cooperative Institute for Meteorological Satellite Studies (CIMSS) provides the RTMA a sky cover product based on geostationary satellite observations and derived products with the best availability possible. As the RTMA combines the HRRR/RAP 1-h forecast field with satellite and *in-situ* surface observations, it provides an ideal representation of an evolving cloud field. For this reason, forecast offices in the NWS Central Region use the RTMA to monitor the quality of their NDFD-gridded sky cover forecasts.[19]

Disclosures

The author has no relevant financial or other potential conflicts of interest to disclose related to the publication of this article.

Acknowledgments

References

1. Office of the Federal Coordinator for Meteorological Services and Supporting Research, "Federal Meteorological Handbook No. 1: surface weather observations and reports," FCM-H1-2005, p. 104 (2005).
2. H. R. Glahn and D. P. Ruth, "The new digital forecast database of the National Weather Service," *Bull. Am. Meteorol. Soc.* **84**, 195–202 (2003).
3. T. M. Hamill et al., "The U.S. National Blend of Models for statistical postprocessing of probability of precipitation and deterministic precipitation amount," *Mon. Weather Rev.* **145**, 3441–3463 (2017).
4. M. S. De Pondeca et al., "The real-time mesoscale analysis at NOAA's National Centers for Environmental Prediction: current status and development," *Weather Forecasting* **26**, 593–612 (2011).
5. NOAA ESRL Global Systems Division, "Experimental model predicts the effect of the 2017 eclipse on weather," *GSD News*, https://www.esrl.noaa.gov/gsd/learn/hotitems/2017/eclipse2017-hrrr.html (2017).
6. M. L. DesJardins, K. F. Brill, and S. S. Schotz, "GEMPAK5 user's guide version 5.0," Technical Report NASA-TM-4260, REPT-91B00036, NAS 1.15:4260, NASA Goddard Space Flight Center, Greenbelt, Maryland (1991).
7. S. Kalluri et al., "From photons to pixels: processing data from the advanced baseline imager," *Remote Sens.* **10**, 177 (2018).
8. T. J. Schmit et al., "A closer look at the ABI on the GOES-R series," *Bull. Am. Meteorol. Soc.* **98**, 681–698 (2017).
9. A. Heidinger, "ABI cloud height," *GOES-R Algorithm Theoretical Basis Document*, NOAA NESDIS STAR, http://www.goes-r.gov/products/ATBDs/baseline/Cloud_CldHeight_v2.0_no_color.pdf (2011).
10. J. J. Gerth, "Sky cover," PhD Dissertation, University of Wisconsin—Madison, 140 p, http://cimss.ssec.wisc.edu/~jordang/work/PhD-Dissertation.pdf (2013).
11. P. Zhu and W. Zhao, "Parameterization of continental boundary layer clouds," *J. Geophys. Res.* **113**, D10201 (2008).
12. J. Smagorinsky, "On the dynamical prediction of large-scale condensation by numerical methods," *Geophys. Monogr.* **5**, 71–78 (1960).
13. C. S. Bretherton, J. R. McCaa, and H. Grenier, "A new parameterization for shallow cumulus convection and its application to marine subtropical cloud-topped boundary layers. Part I: Description and 1D results," *Mon. Weather Rev.* **132**, 864–882 (2004).
14. J. M. Slingo, "The development and verification of a cloud prediction scheme for the ECMWF model," *Q. J. R. Meteorolog. Soc.* **113**, 899–927 (1987).
15. K.-M. Xu and D. A. Randall, "A semiempirical cloudiness parameterization for use in climate models," *J. Atmos. Sci.* **53**, 3084–3102 (1996).
16. H. Sundqvist, E. Berge, and J. E. Kristjansson, "Condensation and cloud parameterization studies with a mesoscale numerical weather prediction model," *Mon. Weather Rev.* **117**, 1641–1657 (1989).
17. S. G. Benjamin et al., "A North American hourly assimilation and model forecast cycle: the rapid refresh," *Mon. Weather Rev.* **144**, 1669–1694 (2016).
18. J. R. Carley, NCWCP, College Park, Maryland, personal communication (2017).
19. J. Wiedenfeld, NWS/CR/WFO, Milwaukee, Wisconsin, personal communication (2017).

Jordan J. Gerth is an associate researcher at the University of Wisconsin–Madison affiliated with the Cooperative Institute for Meteorological Satellite Studies, where he earned his PhD in atmospheric and oceanic sciences in 2013. His primary area of expertise is satellite meteorology. Currently, he works to develop training for, and transition new and experimental satellite products directly to, operational meteorologists in the field as part of the United States satellite proving ground, a government-sponsored readiness activity to prepare operational meteorologists for the next-generation weather satellites.